

Atmospheric and Oceanic Excitations to LOD Change on Quasi-biennial Time Scales *

Li-Hua Ma¹, De-Chun Liao^{1,2} and Yan-Ben Han¹

¹ National Astronomical Observatories, Chinese Academy of Sciences, Beijing 100012; mlh@bao.ac.cn

² Shanghai Astronomical Observatory, Chinese Academy of Sciences, Shanghai 200030

Received 2006 March 14; accepted 2006 April 12

Abstract We use wavelet transform to study the time series of the Earth's rotation rate (length-of-day, LOD), the axial components of atmospheric angular momentum (AAM) and oceanic angular momentum (OAM) in the period 1962–2005, and discuss the quasi-biennial oscillations (QBO) of LOD change. The results show that the QBO of LOD change varies remarkably in amplitude and phase. It was weak before 1978, then became much stronger and reached maximum values during the strong El Nino events in around 1983 and 1997. Results from analyzing the axial AAM indicate that the QBO signals in axial AAM are extremely consistent with the QBOs of LOD change. During 1963–2003, the QBO variance in the axial AAM can explain about 99.0% of that of the LOD, in other words, all QBO signals of LOD change are almost excited by the axial AAM, while the weak QBO signals of the axial OAM are quite different from those of the LOD and the axial AAM in both time-dependent characteristics and magnitudes. The combined effects of the axial AAM and OAM can explain about 99.1% of the variance of QBO in LOD change during this period.

Key words: Earth's variable rotation – atmospheric angular momentum – oceanic angular momentum

1 INTRODUCTION

Earth's variable rotation with its complex state of motion and excitation mechanism that indicates complex overall geodynamical process of the Earth system, reflects interactions among the solid Earth, atmosphere and oceans, etc. In recent decades, some modern space geodetic techniques (such as VLBI, SLR, LLR) have been routinely used to monitor the Earth's variable rotation and provide measurements of unprecedented precision and resolution. This allows for precise checking and studying of the dynamics of the Earth rotation. With the advances in astronomy and earth science, relationship between the variation of Earth's rotation and some geophysical phenomena has attracted wide attention of astronomers, geodesists and geophysicists (for a review, see, e.g., Lambeck 1980; Wahr 1988; Hide & Dickey 1991; Dickey 1995; Zhou et al. 2001; Chao 2004).

Some studies show that the atmosphere is the principal excitation source for length-of-day (LOD) change for periods from a few days up to a few years (Li & Wilson 1988; Dickey 1995; Wilson 1995; Liao & Greiner-Mai 1999). Seasonal oscillations including semiannual and annual changes are the main components of LOD change and are relatively stable. The seasonal components of the axial atmospheric angular momentum (AAM) are consistent with those of LOD change in amplitude and phase (Ma & Han 2006): the annual and semiannual components of the AAM can account for about 95% and 88% of those of LOD change in amplitude, respectively (Yu & Zheng 2000). Gross et al. (2004) studied LOD change and the

* Supported by the National Natural Science Foundation of China.

axial AAM during 1980–2000, and pointed out that zonal winds are the dominant mechanism causing LOD change on intraseasonal, seasonal and interannual time scales. Recently, quasi-biennial oscillation (QBO) present in many geophysical phenomena has begun to attract the attention of some researchers. The period of the QBO varies mainly from about 2.1 years to 2.6 years. Chao (1989) thought that the QBO in LOD change was closely related to the QBO in the stratosphere, and the results of correlation analysis showed that the QBO of atmosphere could excite that of LOD change to a large extent. Liao's result (Liao 2000) showed that main excitation sources of interannual oscillations in LOD change were from atmospheric dynamical processes (including ocean-atmosphere coupling), and the correlation coefficient between LOD change and atmospheric excitation reached 0.6 during 1958–1997. Considering that El Nino/Southern Oscillation (ENSO) and atmospheric QBO can explain interannual variations of LOD change, Zhou & Zheng (1997) pointed out that ENSO events and the atmospheric QBO make large contributions to LOD change on interannual scales. Liu et al. (2005) used wavelet coherence technique to analyze the relationship between LOD change and ENSO events, and showed time-scale-dependent correlations and phase shifts between LOD variations and ENSO events on interannual scales. Zheng et al. (2003) studied the relationships of the LOD, ENSO and the global AAM, and the results revealed the combined effects of multi-scale atmospheric oscillations (including seasonal, quasi-biennial time scales) on the anomalous variations of the interannual LOD change.

In an attempt to understand better the characteristics of LOD change and the couplings among solid Earth, atmosphere and oceans, and especially, atmospheric and oceanic excitations to LOD change on QBO time scales, we use wavelet transform to study the series of LOD change, axial AAM and oceanic angular momentum (OAM), with emphasis on the characteristics and the excitation source of QBO signals in LOD change, and estimate the excitation contribution of axial AAM and OAM on QBO variations of LOD.

2 DATA SETS

2.1 Length of Day

The daily LOD series used in this work is extracted from EOPC04 of the International Earth Rotation and Reference System Service (IERS). The time series covers the period 1962 January 1 to 2005 October 27. In order to remove the high-frequency noise, the data set had been slightly smoothed with Vondrak algorithm by IERS. During the 1960s and 70s, the LOD data were mainly derived from optical astrometric observations. Since the 1980s, the data were mainly obtained from observations made by modern space geodesic techniques with a greatly increased precision. In order to study the contribution by atmospheric and oceanic processes to the excitation of LOD, the effects due to zonal tides for the solid Earth are removed according to IERS conventions 2000. The trend term is also removed before the analysis. The LOD with zonal tide effects removed is usually called “LODR”, but we continue to call it “LOD”, for simplicity, in this paper.

2.2 Atmospheric Angular Momentum

Global atmospheric processes are described by the effective atmospheric angular momentum (EAAM) functions as defined by Equations (1)–(3). The equatorial components (χ_1 and χ_2) of EAAM functions are related to the excitation of polar motion, the axial component (χ_3) is related to the excitation of LOD change, and all three components are composed of a wind term and a mass term. EAAM functions for mass terms are integrated over three whole latitude and longitude grid, and those for wind terms are integrated additionally, over all the pressure layers from the surface to the top of the model. The resulting formulae are as follows (Barnes et al. 1983; Eubanks 1993).

$$\begin{aligned} \chi_1 = \chi_1^p + \chi_1^w = & \frac{-1.098R^4}{(C-A)g} \int_0^{2\pi} \int_{-\pi/2}^{\pi/2} P_s \sin \phi \cos^2 \phi \cos \lambda d\phi d\lambda + \frac{1.5913R^3}{(C-A)\Omega g} \\ & \cdot \int_0^{2\pi} \int_{-\pi/2}^{\pi/2} \int_{P_s}^{P_{\text{top}}} (-u \cos \phi \sin \phi \cos \lambda + v \cos \phi \sin \lambda) dp d\phi d\lambda, \quad (1) \\ \chi_2 = \chi_2^p + \chi_2^w = & \frac{-1.098R^4}{(C-A)g} \int_0^{2\pi} \int_{-\pi/2}^{\pi/2} P_s \sin \phi \cos^2 \phi \sin \lambda d\phi d\lambda + \frac{1.5913R^3}{(C-A)\Omega g} \end{aligned}$$

$$\int_0^{2\pi} \int_{-\pi/2}^{\pi/2} \int_{P_s}^{P_{\text{top}}} (-u \cos \phi \sin \phi \sin \lambda - v \cos \phi \cos \lambda) dp d\phi d\lambda, \quad (2)$$

$$\chi_3 = \chi_3^p + \chi_3^w = \frac{0.753R^4}{C_m g} \int_0^{2\pi} \int_{-\pi/2}^{\pi/2} P_s \cos^3 \phi d\phi d\lambda + \frac{0.998R^3}{C_m \Omega g} \int_0^{2\pi} \int_{-\pi/2}^{\pi/2} \int_{P_s}^{P_{\text{top}}} u \cos^2 \phi dp d\phi d\lambda, \quad (3)$$

where A and C are, respectively, the equatorial and axial moments of inertia of the entire Earth, C_m is the axial moments of inertia of the mantle; R , Ω and g are the mean radius, mean rotation rate and gravity acceleration of the Earth; P_s and P_{top} are the pressures at the surface and the top of model, u and v are the eastward and northward wind velocities, λ and ϕ are the longitude and latitude of the grid point, and the coefficients 1.098, 1.5913 for χ_1 and χ_2 , 0.753 and 0.998 for χ_3 represent the effects of the load deformation, rotational deformation and pole tide on the solid mantle.

The wind term series (χ_3^w) and mass term series (χ_3^p) of the axial AAM for the period 1948 January 1– 2006 December 31, taken every 6 hours, are from the National Centers for Environmental Prediction/National Center for Atmospheric Research (NCEP/NCAR) reanalysis project (Zhou et al. 2005). We use χ_3^w integrated to 10 hPa and χ_3^p with the inverted barometer assumption to form the χ_3 series. The data set is first re-sampled at the same intervals (daily) as the LOD variations by simple averaging, and then with the trend term removed.

In order to study the influence of tropical zonal wind of the axial AAM on LOD, we also analyze the wind terms integrated from surface to 10 hPa and from 100 hPa to 10 hPa for latitude range 30°S–30°N. They are respectively called “tropical wind” and “tropical-stratosphere wind” in this paper. The daily zonal wind series for the period 1980 January – 2003 December is obtained from Japan Meteorological Agency (JMA) (Aoyama et al. 2003).

For further confirmation of the coherence of the ENSO events to the QBO in LOD, the Southern Oscillation Index (SOI) at one month interval for 1977–2005, downloaded from website of the Climate Prediction Center, is also analyzed.

2.3 Oceanic Angular Momentum

The OAM series used in this work is the results of a simulation of the general circulation of the oceans done at JPL (Gross et al. 2005). The ocean model used in this simulation is based on the MIT ocean general circulation model and has realistic boundaries and bottom topography (Marshall et al. 1997a, b). With 46 vertical levels ranging in thickness from 10 m at the surface to 400 m at depths and using height as the vertical coordinate, the model spans the globe between 78°S to 80°N latitude with a latitudinal grid-spacing ranging from 1/3 degree at the equator to 1 degree at high latitudes and a longitudinal grid-spacing of 1 degree. The model is subsequently forced with the 1949–2002 surface fluxes (twice daily wind stress, daily surface heat flux and evaporation-precipitation fields) from the NCEP/NCAR reanalysis project. Similar to AAM, OAM has three components for a mass term (bottom pressure) and a motion term (current). The data set covers the period 1947 January– 2002 December, at 10 day intervals. The axial component of OAM is related to LOD variation, while the trend terms of the axial OAM are removed before the analysis.

3 ANALYSIS

3.1 Wavelet Transform

Fast Fourier Transform (FFT) is a useful tool to study the power spectrum of stationary time series. The distribution of spectral density from FFT identifies the energy associated with each frequency, but it does not give any information about localization in the time series. Recently, wavelet transform has become a common tool for analyzing localized variations of power within time series. By decomposing the time series into the time-frequency space, this technique lays out time-dependent information of the signals in both the time and frequency domains. So, wavelet analysis method is adapted to non-stationary time series. Wavelet transform has been used in numerous studies in geophysics, astronomy and other fields. Details

on wavelet transform have been given by various authors (Daubechies 1992; Kumar & Foufoula-Georgiou 1997; Torrence & Compo 1998; Zhou & Zheng 2000). With wavelet transform, variable characteristics of QBO signal along with time can be clearly revealed, and in this work the Morlet wavelet, in particular, is used as the base wavelet.

3.2 Data Analysis and Comparison

When analyzing the series of LOD change, axial AAM and OAM, in order to reduce the influence of edge-effects of wavelet transform, a statistical method (Zheng et al. 2000) is used to extrapolate the data series for three years at the two ends, and after the wavelet transform the results are truncated to the original length. The results of LOD change are shown in Figure 1, which comprise four panels with different contents. The original LOD series with the trend term and zonal tide effects removed is given in Figure 1(a); Figure 1(b) displays localized wavelet spectra of LOD change. Considering that variable characteristics and excitation mechanism of LOD change on QBO time scales are studied in this work, wavelet scales are from 1.4-year to 3.2-year with spectra lined out with contour in the figure. In order to see clearly the general distribution of the spectral power of the QBO as given by the usual Fourier spectrum, the global wavelet power spectrum is calculated and shown in Figure 1(c), which actually is a time-average of the wavelet power spectrum for each scale/frequency. In order to quantitatively estimate of the QBO signals, scale-average of the wavelet spectra over 1.6–2.9 years is made for each epoch of time and the results are plotted in Figure 1(d).

Similar to LOD change, wavelet analysis of the axial AAM and OAM is shown in Figures 2 and 3, with the same four panels in each.

Figures 1(b) and 2(b) display clearly the time-dependent characteristics of LOD change and axial AAM on QBO time scales. During 1962–2005, the time-dependent structures in the axial AAM are very similar to those in the LOD change. Their spectral densities of QBO reach maxima around 1983 and 1997, respectively, which clearly correspond to the very strong El Nino events happening in those times. Meanwhile, comparing Figures 1(c) with 2(c), their global power spectra of the QBO are concentrated on periods around 2.4 years with power of about $7\sim 8 \text{ ms}^2$. The scale-averaged QBO variation shows their time-dependent characteristics clearly in Figures 1(d) and 2(d). Considering that there exist end-effects in the wavelet transforms before 1963 and after 2003, we analyze their subsets during 1963–2003. Comparing Figures 1(d) with 2(d), their time-dependent characteristics of QBO are clearly seen to be similar to each other. The mean variances are about 0.007097 ms^2 for LOD change, and 0.006852 ms^2 for the axial AAM. Using this scale-averaged QBO variance, the time-dependent amplitudes of the QBO can be estimated. As shown in Figure 4(a), the amplitude and variable characteristics of LOD change are well consistent with those of the axial AAM. Using these results, a simple calculation shows that the QBO in axial AAM can explain about 99.0% of the variance of the QBO in the LOD. It strongly suggests that almost all of the changes of LOD on QBO time scales are excited by the QBO in the axial AAM.

Under conservation of angular momentum for the whole Earth system, the effects of the axial OAM can give rise to LOD change (Johnson et al. 1999; Ponte et al. 2000, 2002). Comparing Figure 3(b) with Figures 1(b) and 2(b) one can see that the QBO features for the axial OAM are quite different from those for the LOD and axial AAM. The spectral power of the QBO for the OAM shown in Figure 3(c) is concentrated on periods around 1.9 years, in contrast to around 2.4 years for axial AAM and LOD change. It should be emphasized that the magnitude of the QBO power spectra for axial OAM is much less than those for LOD and axial AAM by a factor of 10^{-3} . Again, the scale-averaged QBO variance for OAM in Figure 3(d) is quite different from those for LOD and AAM in both time-dependent characteristics and magnitudes. It is very interesting to note that of the three areas with the highest spectral energies in Figure 3(b) (the three peaks in Figure 3(d)) two of them clearly correspond to the strong La Nina events happening around 1973–1976 and 1988–1989. It strongly suggests that although the QBO components in OAM are a lot weaker than those in AAM, their contributions to the occurrence of La Nina events should be non-negligible. Figure 4(b) compares the amplitude of the QBO signal in OAM (dashed line, right scale) with the difference $\text{QBO}(\text{LOD}) - \text{QBO}(\text{AAM})$ (full line, left scale). It should be pointed out that the scale for QBO(OAM) in Figure 4(b) is enlarged by a factor of 2 in order to show up its variation. By comparison of the two curves the different features of the QBO in OAM and those in LOD and AAM are clearly seen. Calculation indicates that the total QBO signals in the axial OAM and AAM can explain about 99.1% of the QBO variance in LOD change in the period 1963–2001. Because of the different features of the two curves in Figure 4(b), the

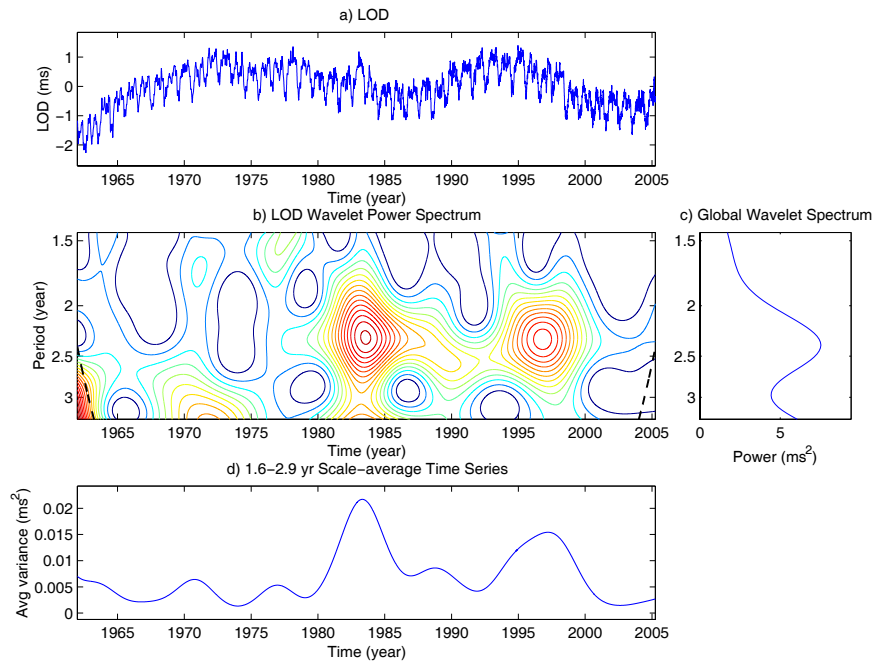


Fig. 1 LOD data series for the period 1962–2005 and the corresponding wavelet power spectra. (a) LOD series; (b) Localized wavelet power spectrum of the LOD series. The left axis is the Fourier period (in years) corresponding to the wavelet scale and the bottom axis is time (in years). The dotted line shows the border of edge-effects of the Morlet wavelet transform, outside of this border the wavelet spectra are doubtful; (c) Global wavelet spectrum; (d) Scale-average of the wavelet spectrum over Fourier periods 1.6 to 2.9 years;

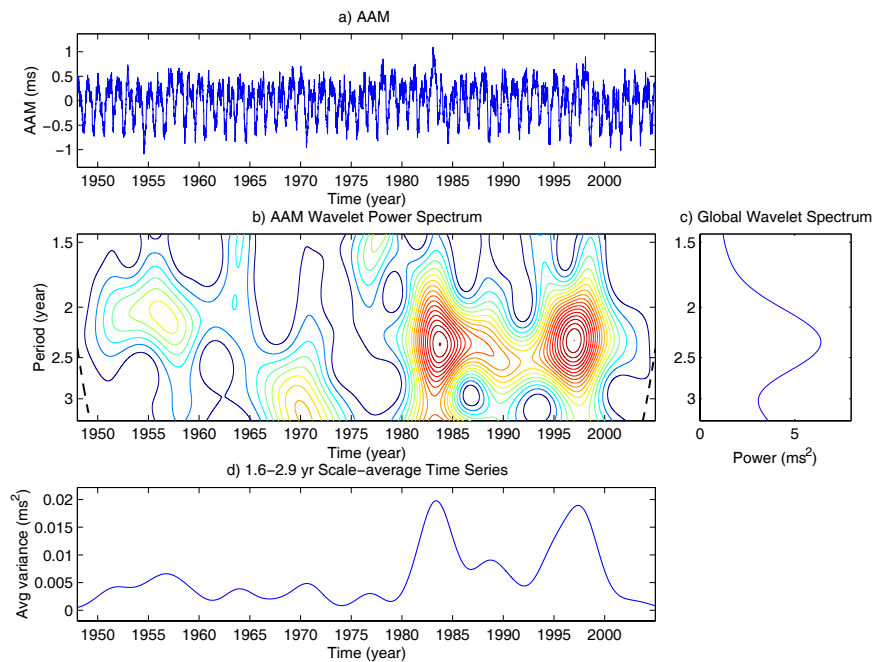


Fig. 2 Axial AAM data series for the period 1948–2004 and corresponding wavelet power spectra. The meaning of the four panels is the same as in Fig. 1.

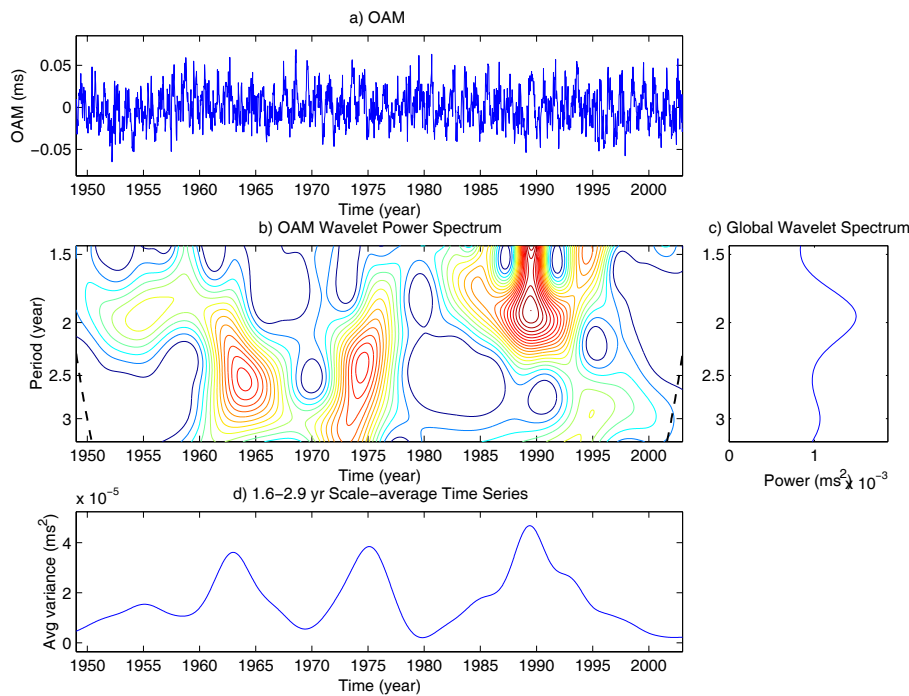


Fig. 3 Axial OAM data series during 1949–2003 and corresponding wavelet power spectra. The meaning of the four panels is the same as in Fig. 1.

variance of $\text{QBO}(\text{LOD}) - \text{QBO}(\text{AAM}) - \text{QBO}(\text{OAM})$ slightly increases from 0.000066 ms^2 of the variance of $\text{QBO}(\text{LOD}) - \text{QBO}(\text{AAM})$ to 0.000073 ms^2 in the period 1963–2001.

From above analysis, one can see that the excitation of LOD change on QBO time scales is mainly from the axial AAM, while that from the axial OAM is very small.

4 SUMMARY AND DISCUSSION

Results from the wavelet analysis show there are present time-dependent features in the QBOs of LOD change, axial AAM and OAM and that, in particular, there is good consistency between the QBOs of LOD change and axial AAM, both in amplitude and phase. On this time scale, QBO (AAM) can explain most (99.0%) of the variance of the LOD scale; while $\text{QBO}(\text{AAM}) + \text{QBO}(\text{OAM})$ can explain even more (about 99.1%) of the LOD variance of the LOD, for the period 1963–2001. The unexplained part (less than 1%) of the QBO variance in LOD may be caused by some other excitation sources, such as hydrological processes, etc.

Chao (1989) analyzed interannual LOD change and QBO signals in equatorial stratosphere wind, and showed that the QBO in equatorial stratosphere wind could account for about 0.064 ms of the interannual LOD variation for the period 1964–1987. From Figure 4(a) above the estimated $\text{QBO}(\text{AAM})$ contribution is about 0.076 ms for 1963–2003 and 0.077 ms for 1963–2001, while from Figure 4(b) the estimated $\text{QBO}(\text{OAM})$ contribution is only 0.004 ms for 1963–2001, which is about 1/20 of the $\text{QBO}(\text{AAM})$ contribution. Gross et al. (2004) estimated the axial OAM and AAM contributions to the variance of the interannual LOD for 1980–2000 are, respectively, 0.8% and 87.3%, with the former less than one percent of the latter. These results further confirm that the oceanic contribution to LOD is very small on both QBO and interannual time scales.

As is known to all, global wind on seasonal time scale is dominated by tropical wind. In order to investigate contribution of tropical wind to axial AAM and hence to LOD on QBO time scales, we have made

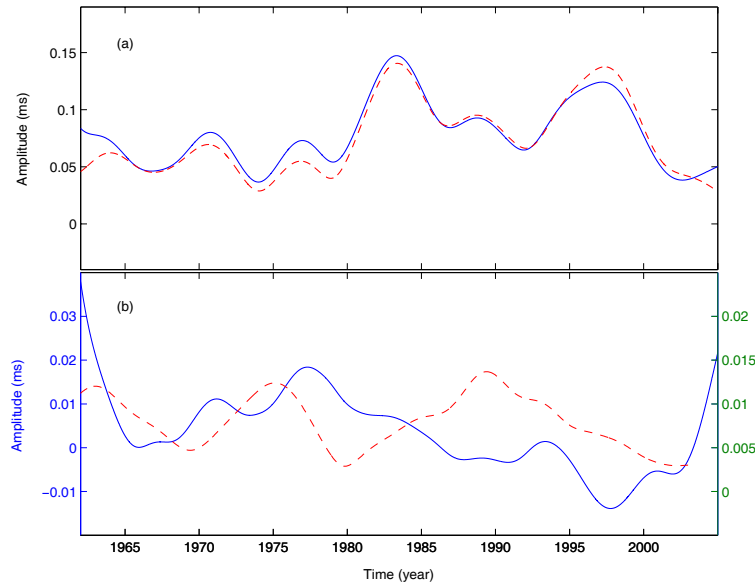


Fig. 4 Scale-average amplitudes of QBOs in LOD change, axial AAM and OAM. (a) Amplitudes of the QBO signals in LOD (full lines) and in AAM (dashed lines); (b) Differences in amplitudes, QBO(LOD) – QBO(AAM) (full lines) and the amplitude of QBO(OAM) (dashed lines).

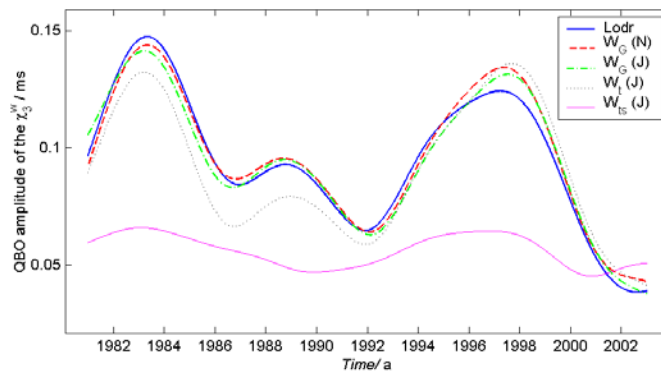


Fig. 5 Amplitudes of the QBO components in LOD (thick solid line), global winds of the axial AAM (NCEP) (dashed line) and AAM (JMA) (dash-dotted line), tropical wind (dotted line) and tropical stratospheric wind (thin solid line) of the AAM (JMA) as given by scale-average of the wavelet spectra for 1981–2002.

further analysis of the global winds in axial AAM(NCEP) and AAM(JMA), tropical wind and tropical-stratospheric wind of the axial AAM(JMA). Amplitudes of the QBO components in global winds of axial AAM(NCEP) and AAM(JMA) given by scale-averages of their wavelet spectra are shown in Figure 5 and compared with that of the QBO components in LOD for 1981–2002. One can see that the QBO components in global winds of both AAM(NCEP) and AAM(JMA) are in good agreement with those in LOD. As pointed out by Aoyama & Natio (2000), there is only a small difference in the wind terms of the axial AAM between the JMA and NCEP models. Further calculation shows that the global winds of AAM(NCEP) and AAM(JMA) can respectively explain about 95.6% and 95.3% of the amplitudes of the LOD on QBO

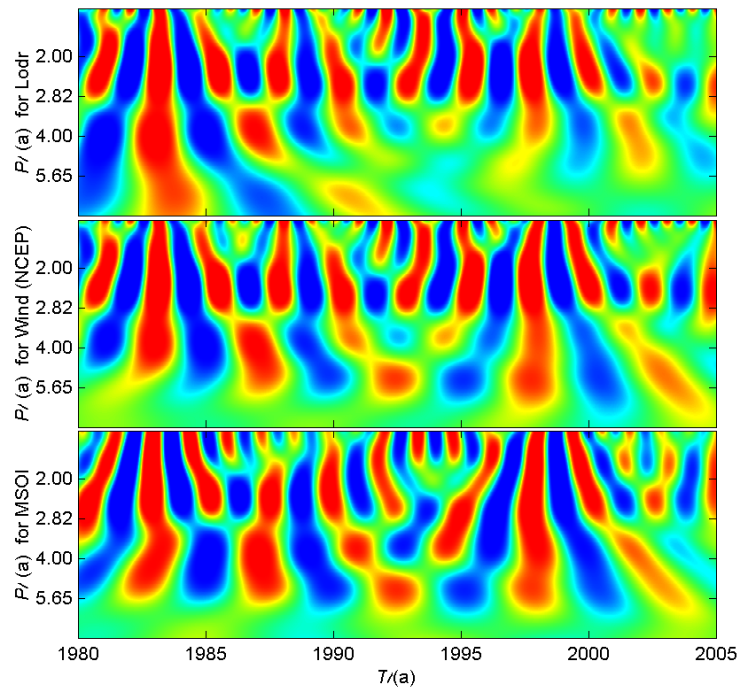


Fig. 6 Wavelet amplitude spectra of LOD (top), global zonal wind (middle) and MSOI (bottom) on interannual time scale during 1980–2004. Red for positive polarity, blue for negative. Depth of colour is a measure of the size of spectral energy.

time scales in the period 1981–2002. Also shown in Figure 5 are the QBO components in tropical and tropical-stratospheric winds of AAM(JMA), and they can respectively explain about 88.2% and 54.4% of the QBO amplitudes of the LOD during the same period. As for the QBO amplitudes of the tropical wind, about 56.6% comes from the tropical-stratospheric wind in the period concerned. From these comparisons it is strongly suggested that the QBO changes of the global wind term of the axial AAM are dominated by contributions from variations of the tropical zonal wind, and a large part of the amplitude changes of the tropical wind is from the tropical-stratosphere wind.

Some studies show close relations between earth's variable rotation and ENSO events (e.g. Chao 1989; Zheng et al. 1990; Zhou et al. 2001; Han et al. 2002). Dickey et al. (1994) showed the bimodal concentration around 4.3 years and 2.3 years of ENSO events in LOD, SOI and AAM. Dickey et al. (1994) and Chao & Natio (1995) also argued that there was phase coherence between ENSO events and the QBO in LOD, SOI and AAM. To further confirm this phenomenon, Figure 6 shows the wavelet amplitude spectra of the LOD, global winds in axial AAM(NCEP) and modified SOI series for 1980–2004, in which polarities and phases of the two main quasi-periodic components are shown clearly. Instances of coherence of the polarities and phases of the two quasi-periodic components with ENSO events are listed in Table 1. From Figure 6 and Table 1 one can see that strong El Nino/La Nina events always happen in cases when the polarities of the two quasi-periodic components are both in positive/negative phase and their intensities are both strong, while medium and weak ENSO events occur when their polarities and phases are not the same or their intensities are relatively weak. One also can see from Figure 6 that around the years 1982–1983 and 1997–1998 of strong El Nino events, the QBO intensities are obviously stronger than in other times.

In addition, QBO signal in the stratosphere was discovered in 1950s, but its origin remained unclear for some time. Atmospheric QBO is mainly contributed by the equatorial zonal wind from fluctuations between the easterlies and westerlies. In recent years, gravity waves have come to be seen as a major contributor to

Table 1 Coherence of the ENSO events occurred during 1980–2004 with the polarities and phases of the bimodalities at interannual time scale ('transit' means the polarity in transit from one to the other; 'P' for polarity and 'I' for intensity).

Time (year)	ENSO status	P (QBO)	I (QBO)	P (~4.3a)	I (~4.3a)	Coherence
1982–1983	strong El Nino	positive	strong	positive	strong	in phase
1986–1987	mid- El Nino	negative	strong	positive	strong	not in phase
1988–1989	strong La Nina	negative	strong	negative	strong	in phase
1991–1992	mid-El Nino	negative	mid-strong	positive	weak	not in phase
1994–1995	mid-El Nino	transit	strong	positive	weak	not in phase
1997–1998	strong El Nino	positive	strong	positive	mid-strong	in phase
1998–2000	mid-La Nina	negative	strong	transit	weak	not in phase
2002–2003	mid-El Nino	positive	mid-strong	transit	mid-strong	not in phase

the QBO. Effects of the QBO include mixing of stratospheric ozone by the secondary circulation caused by the QBO, modification of monsoon precipitation, and influence on stratospheric circulation in northern hemisphere winter. Some studies showed that atmospheric QBO was related to some geophysical phenomena, such as solar cycle (Soukharev 1997; Labitzke 2005), ozone variability (Soukharev 1999), and east African seasonal rainfall (Indeje & Semazzi 2000). Results of this paper would be helpful to further studies on the origin and variation of atmospheric QBO and a deeper understanding of the variation mechanism of Earth rotation.

Acknowledgements The authors are grateful to IERS, NCEP and JMA for respectively providing EOPC04, OAM and AAM data series. Wavelet software is provided by C. Torrence and G. Compo, and is available at URL: <http://paos.colorado.edu/research/wavelets/>. The authors grateful acknowledge an anonymous referee for helpful suggestions. The study is supported by the National Natural Science Foundation of China under Grant 10373017.

References

- Aoyama Y., Naito I., 2000, *J. Geophys. Res.*, 105, D10, 12417
Aoyama Y., Naito I., Iwabuchi T. et al., 2003, *Earth Planets Space*, 55, e25
Barnes R. T. H., Hide R., White A. A. et al., 1983, *Proc R Soc Lond A*, 387, 31
Chao B. F., 1989, *Science*, 243, 923
Chao B. F., 2004, ed. Nancy R. Vandenberg and Karen D. Baver, NASA/CP-2004- 212255
Chao B. F., Naito I., 1995, *EOS, Trans. Amer. Geophys. Union*, 76, 161
Daubechies I., 1992, Philadelphia: SIAM
Dickey J. O., 1995, Washington: AGU, p.356
Dickey J. O., Marcus S. L., Hide R. et al., 1994, *J. Geophys. Res.*, 99, 23921
Eubanks T. M., 1993, *Geodyn, Ser.*, 24. Smith DE and Turcotte DL eds. Washington DC: AGU, p.1
Gross R. S., Fukumori I., Menemenlis D. et al., 2004, *J. Geophys. Res.*, 109, B01406
Gross R. S., Fukumori I., Menemenlis D. et al., 2005, *J. Geophys. Res.*, 110, B09405
Han Y. B., Zhao J., Li Z. A., 2002, *Chin. Sci. Bull.*, 47(2), 105
Hide R., Dickey J. O., 1991, *Science*, 253, 629
Indeje M., Semazzi F. H. M., 2000, *Meteorol. Atmos. Phys.*, 73, 227
Johnson T. J., Wilson C. R., Chao B. F., 1999, *J. Geophys. Res.*, 104, 25183
Kumar P., Foufoula-Georgiou E., 1997, *Rev. Geophys.*, 35(4), 385
Labitzke K., 2005, *J. Atmos. Sol.-Terr. Phys.*, 67, 45
Lambeck K., 1980, Cambridge: Cambridge Univ. Press
Li Z. A., Wilson C. R., 1988, *Chin. Astron. Astrophys.*, 12, 48
Liao D. C., 2000, *Acta. Astronomica Sinica*, 41(2), 139
Liao D. C., Greiner-Mai H., 1999, *J. Geodesy*, 73, 466
Liu L.T., Hsu H. T., Grafarend E. W., 2005, *J. Geodyn.*, 39(3), 267
Ma L. H., Han Y. B., 2006, *Chin. J. Astron. Astrophys. (ChJAA)*, 6, 120

- Marshall J., Adcroft A., Hill C. et al., 1997b, *J. Geophys. Res.*, 102, C3, 5753
Marshall J., Hill C., Perelman L. et al., 1997a, *J. Geophys. Res.*, 102, C3, 5733
Ponte R. M., Rajamony J., Gregory J. M., 2002, *Clim. Dyn.*, 19, 181
Ponte R. M., Stammer D., 2000, *J. Geophys. Res.*, 105, 17161
Soukharev B., 1997, *Ann. Geophysicse*, 15, 1595
Soukharev B., 1999, *J. Atmos. Sol.-Terr. Phys.*, 61, 1093
Torrence C., Compo G., 1998, *Bull. Amer. Meteor. Soc.*, 79, 61
Wahr J. M., 1988, *Ann. Rev. Earth Planet. Sci.* 16, 231
Wilson C. R., 1995, *Rev. Geophys.*, 33(S), 225
Yu N. H., Zheng D. W., 2000, *Chin. Astron. Astrophys.*, 24, 495
Zheng D. W., Chao B. F., Zhou Y. H. et al., 2000, *J. Geodesy*, 74, 249
Zheng D. W., Ding X. L., Zhou Y. H. et al., 2003, *Glob. Planet. Change*, 36, 89
Zheng D. W., Song G. X., Luo S. F., 1990, *Nature*, 348, 119
Zhou Y. H., Salstein D. A., Chen J. L., 2006, *J. Geophys. Res.*, 111, D12108
Zhou Y. H., Zheng D. W., 1997, *Acta. Astronomica Sinica*, 38(2), 209
Zhou Y. H., Zheng D. W., 2000, *Chinese Journal of Computational Physics*, 17(2), 209
Zhou Y. H., Zheng D. W., Liao X. H., 2001, *J. Geodesy*, 75, 164
Zhou Y. H., Zheng D. W., Yu N. H. et al., 2001, *Chin. Sci. Bull.*, 46(11), 881